

## **WAVELET ANALYTIC NON-STATIONARY SEISMIC RESPONSE OF TANKS**

Pranesh Chatterjee\* and Biswajit Basu\*\*

\*Department of Civil Engineering, K.U. Leuven  
3001 Heverlee, Belgium

\*\*Department of Civil, Structural and Environmental Engineering  
Trinity College, Dublin 2, Ireland

### **SUMMARY**

A wavelet analytic technique has been developed for the non-stationary seismic response of fixed-base liquid storage tanks. The ground acceleration has been characterized through estimates of statistical functionals of wavelet coefficients generated from a single accelerogram of a ground motion process. The tank-liquid system has been modeled as a two-degree-of-freedom (2-DOF) system. Both sloshing and impulsive actions of the tank liquid are considered. The wavelet domain dynamic equations have been formulated and solved to find out the coefficients of hydrodynamic pressure on the tank wall, base shear, and overturning moment at the tank base. Closed form expression for the instantaneous power spectral density function (PSDF) of the response quantities in terms of the functionals of the input wavelet coefficients has been obtained. The moments of this PSDF are used to estimate the expected largest peak coefficients of the hydrodynamic pressure, base shear and base moment developed in the tank. Parametric variations are carried out to study the effects of the height of liquid in tank and the ratio of liquid height to tank radius on the tank responses.

**KEYWORDS:** Storage Tank, Non-stationary, Seismic Response, Wavelet

### **INTRODUCTION**

The effect of seismic excitations on liquid storage tanks has been studied by several researchers in the past. The storage tanks of oil and petrochemical industries, water treatment plants and nuclear spent-fuel assemblies are particularly subjected to the risk of damage due to earthquake-induced vibrations. Seismic ground motions induce hydrodynamic pressure on the tank wall and also induce shear and overturning moment at the tank base. These may cause increase in stresses in the tank wall, thereby damaging the tanks. For these reasons, the fluid storage tanks subjected to strong ground excitations need a thorough investigation. Further, the responses of tanks to seismic excitations become complex, as the ground motions are non-stationary in nature with both amplitude and frequency non-stationarities (e.g., see Basu and Gupta (1998)).

The responses of fluid storage tanks have been studied by several researchers, both theoretically and experimentally. Housner (1963) proposed the values for equivalent masses with their locations to represent the forces and moments exerted by the liquid on the tank. Veletsos and Yang (1977) used Rayleigh-Ritz method to predict the natural frequencies of the tank-liquid system. Haroun (1983) carried out detailed theoretical analysis of dynamic behaviour of coupled liquid-shell system for rigidly anchored tanks under vertical seismic excitations. Haroun and Tayel (1985) considered fixed tanks to evaluate the effect of base fixation on tank behaviour due to vertical seismic excitations. However, it has been seen that the responses induced or the axial stresses developed in tanks due to vertical component of earthquake excitation are much smaller than those due to the horizontal component of ground motion. The studies performed by Peek (1988) and Peek and Jennings (1988) concentrated on the tank behaviour due to lateral loads. Veletsos and Tang (1990) have shown the effects of impulsive and convective actions of the liquid on the tank responses, and considered the horizontal and rocking motions of the foundation. Koh et al. (1998) studied the dynamic response, including sloshing motion, of the tanks subjected to lateral excitations by modeling the tank structure by finite element method and the fluid region by indirect boundary element method. In all these studies, the loadings were either considered to be harmonic or represented by deterministic time histories, whereas seismic excitations are known to be random in nature

with both amplitude and frequency non-stationarities. These non-stationarities may considerably affect the structural responses, as shown by Yeh and Wen (1990) and Basu and Gupta (1997, 1998, 1999, 2000a).

In the present study, the non-stationary response of fixed-base liquid storage tanks subjected to lateral component of seismic base accelerations has been formulated. A wavelet analytic stochastic vibration analysis is proposed in this paper by using the formulation of Basu and Gupta (1998). Wavelet-based studies have been used for identification of linear and non-linear systems and for solving partial differential equations by Ghanem and Romeo (2000, 2001). Wavelets have also been used for representation of stochastic forces and simulation of random fields by Zeldin and Spanos (1996). Basu and Gupta (1998) and Mukherjee and Gupta (2002a, 2002b) worked on the characterization of ground motions based on wavelets. Wavelet-based spectrum-compatible ground motions have been generated by Mukherjee and Gupta (2002b). The time-frequency localization property of wavelets can be appropriately used to extract information about the contribution of a particular frequency locally in time in a signal on any desired scale, broad or narrow, which would not be possible by Fourier domain analysis or even by short-time (windowed) Fourier transform-based analysis. The fixed-base tank-liquid structural system with impulsive and convective modes of vibrating liquid is modeled as a two degree of freedom (2-DOF) system. Each of the vibrating modes of the liquid is represented by a linear spring and a linear viscous damper. The ground motion is characterized in terms of certain statistical functionals of the wavelet coefficients of the ground acceleration time history (see Basu and Gupta (1998)). The functionals of the wavelet coefficients are obtained from a single realization of time history of a ground motion process by applying statistical techniques (see Chatterjee and Basu (2001)). The expected response spectra are computed by stochastic wavelet theory (Basu and Gupta, 1998) from these processed wavelet coefficients for two damping ratios, and are compared with ensemble averages of time history integration results. A parametric study has been carried out to observe the effects on the tank responses by varying the liquid height in the tank and the height-radius ratio of the tank.

The proposed approach can be used to obtain the stochastic response of liquid storage tanks under seismic excitations for any desired response function with a level of confidence. This approach has the advantage of avoiding the time history simulation computations, particularly when few time histories are available from a site and are difficult to generate synthetically. Further, the ground motion non-stationarities (both amplitude and frequency) are taken into account in this procedure. Also, the modal interaction is exactly incorporated in the formulation unlike the spectrum superposition techniques.

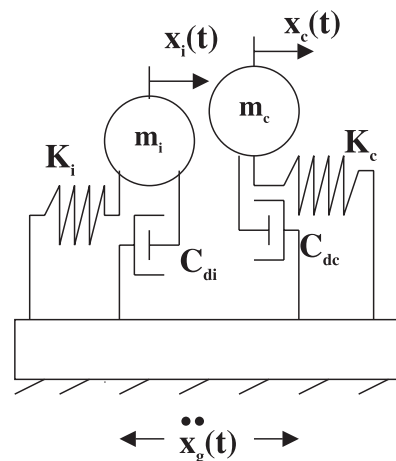


Fig. 1 2-DOF model of the tank-liquid-foundation system

## FORMULATION

### 1. Modeling of the System

The superstructure consists of a right circular cylindrical, rigid thin-walled tank of radius,  $R$ , filled with an incompressible liquid of density,  $\rho_l$ , to a height,  $H$ , and is assumed to be rigidly fixed to a thick, rigid, circular mat, which is of the same radius as that of the tank. The tank wall is assumed to be of

uniform thickness,  $h$ . The Young's modulus of elasticity and the density of the tank material are denoted by  $E$  and  $\rho$ , respectively. The tank with the mat is anchored to the ground surface. The liquid in the tank is assumed to vibrate in the impulsive as well as in the convective mode. The tank-liquid system is represented by mass-spring-dashpot model. The impulsive mass of the liquid,  $m_i$ , is assumed to be connected to the fixed-base of the tank through a linear spring with stiffness,  $K_i$ , and a linear viscous damper with coefficient,  $C_{di}$ . The convective mass of the liquid,  $m_c$ , is also assumed to be connected to the fixed-tank base through a linear spring with stiffness,  $K_c$ , and a linear viscous damper with coefficient,  $C_{dc}$ .  $\zeta_i$  and  $\zeta_c$  respectively denote the damping ratios of the impulsive and convective modes of the liquid. The impulsive mass of the liquid moves in unison with the tank wall, and hence, its natural frequency,  $\omega_i$ , may be considered to be the same as the natural frequency of the tank,  $\omega_n$ . The convective part of the liquid may be assumed to be vibrating in the fundamental sloshing mode with natural frequency,  $\omega_c$ . The rocking motions of the system may be ignored due to fixity at the tank base. The schematic diagram of the dynamical mass-spring-dashpot model adopted to represent the tank-liquid system is shown in Figure 1.

**2. Equations of Motion**

Let the tank-fluid system, as described earlier, be subjected to a horizontal free-field seismic ground displacement,  $x_g(t)$ . The displacements of the impulsive and convective masses of the liquid in the tank relative to the ground surface are denoted by  $x_i(t)$  and  $x_c(t)$ , respectively. On considering only the impulsive motion of the liquid, one may get

$$m_i \ddot{x}_i(t) + C_{di} \dot{x}_i(t) + K_i x_i(t) = -m_i \ddot{x}_g(t) \tag{1}$$

On dividing both sides of Equation (1) by  $m_i$  and on using the relations,  $\frac{K_i}{m_i} = \omega_i^2$  and  $\frac{C_{di}}{m_i} = 2\zeta_i \omega_i$ , we obtain

$$\ddot{x}_i(t) + \omega_i^2 x_i(t) + 2\zeta_i \omega_i \dot{x}_i(t) = -\ddot{x}_g(t) \tag{2}$$

Similarly, on considering only the convective motion of the liquid, one may obtain

$$m_c \ddot{x}_c(t) + C_{dc} \dot{x}_c(t) + K_c x_c(t) = -m_c \ddot{x}_g(t) \tag{3}$$

On dividing both sides of Equation (3) by  $m_c$ , and on using the relations,  $\frac{K_c}{m_c} = \omega_c^2$  and  $\frac{C_{dc}}{m_c} = 2\zeta_c \omega_c$ , we obtain

$$\ddot{x}_c(t) + \omega_c^2 x_c(t) + 2\zeta_c \omega_c \dot{x}_c(t) = -\ddot{x}_g(t) \tag{4}$$

The overdots in the above equations denote differentiations with respect to time. The expressions for  $\omega_i$  ( $= \omega_n$ ), i.e. for the impulsive mode, and for  $\omega_c$ , i.e. for the first sloshing mode, are respectively given by (Veletsos and Tang, 1990)

$$\omega_i = \omega_n = \frac{C_i}{H} \sqrt{\frac{E}{\rho}} \tag{5}$$

and

$$\omega_c = 2\pi \sqrt{\lambda_1 \tanh\left(\lambda_1 \frac{H}{R}\right) \frac{g}{R}} \tag{6}$$

where,  $g$  is the acceleration due to gravity, and  $\lambda_1$  is the first root of the first derivative of Bessel function of first kind and first order. The set of differential equations given by Equations (2) and (4) may be solved to obtain the non-stationary response of the tank-fluid system based on wavelet analytic techniques for seismic base acceleration,  $\ddot{x}_g(t)$ , with known non-stationary statistical characteristics in terms of wavelet coefficients. In the following sections, the non-stationary seismic response of the tank-

liquid system has been obtained by extending the wavelet-based formulation of Basu and Gupta (1998) for dynamical systems. A discussion on the wavelet basis used is presented in Appendix A.

### 3. Stochastic Formulation

The structural response functions may as well be represented in a similar way in terms of wavelet functionals, as discussed above for the case of base acceleration function,  $\ddot{x}_g(t)$ . On following Equation (A.1), the displacements of impulsive and convective masses of the liquid may be expanded in terms of wavelet coefficients respectively as

$$x_i(t) = \sum_i \sum_j \frac{K'' \Delta b}{a_j} W_\psi x_i(a_j, b_i) \psi_{a_j, b_i}(t) \quad (7)$$

and

$$x_c(t) = \sum_i \sum_j \frac{K'' \Delta b}{a_j} W_\psi x_c(a_j, b_i) \psi_{a_j, b_i}(t) \quad (8)$$

On substituting the expressions for  $x_i(t)$ ,  $x_c(t)$  and  $\ddot{x}_g(t)$  from Equations (A.1), (7) and (8) in Equations (2) and (4) respectively, we obtain

$$\begin{aligned} & \sum_i \sum_j \frac{K'' \Delta b}{a_j} W_\psi x_i(a_j, b_i) \ddot{\psi}_{a_j, b_i}(t) + 2\zeta_i \omega_i \sum_i \sum_j \frac{K'' \Delta b}{a_j} W_\psi x_i(a_j, b_i) \dot{\psi}_{a_j, b_i}(t) \\ & + \omega_i^2 \sum_i \sum_j \frac{K'' \Delta b}{a_j} W_\psi x_i(a_j, b_i) \psi_{a_j, b_i}(t) + \sum_i \sum_j \frac{K'' \Delta b}{a_j} W_\psi \ddot{x}_g(a_j, b_i) \psi_{a_j, b_i}(t) = 0 \end{aligned} \quad (9)$$

and

$$\begin{aligned} & \sum_i \sum_j \frac{K'' \Delta b}{a_j} W_\psi x_c(a_j, b_i) \ddot{\psi}_{a_j, b_i}(t) + 2\zeta_c \omega_c \sum_i \sum_j \frac{K'' \Delta b}{a_j} W_\psi x_c(a_j, b_i) \dot{\psi}_{a_j, b_i}(t) \\ & + \omega_c^2 \sum_i \sum_j \frac{K'' \Delta b}{a_j} W_\psi x_c(a_j, b_i) \psi_{a_j, b_i}(t) + \sum_i \sum_j \frac{K'' \Delta b}{a_j} W_\psi \ddot{x}_g(a_j, b_i) \psi_{a_j, b_i}(t) = 0 \end{aligned} \quad (10)$$

Now, on Fourier transforming both sides of Equations (9) and (10), premultiplying both Equations (9) and (10) by  $\hat{\psi}_{a_k, b_l}^*(\omega)$ , and then on using the relation (see Basu and Gupta, 1998),

$$\hat{\psi}_{a_j, b_i}(\omega) \hat{\psi}_{a_k, b_l}^*(\omega) = \delta_{jk} \hat{\psi}_{a_j, b_i}(\omega) \hat{\psi}_{a_k, b_l}^*(\omega) \quad (11)$$

we get

$$\begin{aligned} & \sum_i W_\psi x_i(a_j, b_i) \hat{\psi}_{a_j, b_i}(\omega) [-\omega^2] + \sum_i W_\psi x_i(a_j, b_i) \hat{\psi}_{a_j, b_i}(\omega) [2i\zeta_i \omega_i \omega] \\ & + \sum_i W_\psi x_i(a_j, b_i) \hat{\psi}_{a_j, b_i}(\omega) [\omega_i^2] + \sum_i W_\psi \ddot{x}_g(a_j, b_i) \hat{\psi}_{a_j, b_i}(\omega) = 0 \end{aligned} \quad (12)$$

and

$$\begin{aligned} & \sum_i W_\psi x_c(a_j, b_i) \hat{\psi}_{a_j, b_i}(\omega) [-\omega^2] + \sum_i W_\psi x_c(a_j, b_i) \hat{\psi}_{a_j, b_i}(\omega) [2i\zeta_c \omega_c \omega] \\ & + \sum_i W_\psi x_c(a_j, b_i) \hat{\psi}_{a_j, b_i}(\omega) [\omega_i^2] + \sum_i W_\psi \ddot{x}_g(a_j, b_i) \hat{\psi}_{a_j, b_i}(\omega) = 0 \end{aligned} \quad (13)$$

Equations (12) and (13) may further be simplified to obtain the explicit expressions of wavelet transform coefficients of  $x_i$  and  $x_c$  in terms of wavelet transform coefficient of  $\ddot{x}_g$  as

$$\sum_i W_\psi x_i(a_j, b_i) \hat{\psi}_{a_j, b_i}(\omega) = H_i(\omega) \sum_i W_\psi \ddot{x}_g(a_j, b_i) \hat{\psi}_{a_j, b_i}(\omega) \quad (14)$$

and

$$\sum_i W_\psi x_c(a_j, b_i) \hat{\psi}_{a_j, b_i}(\omega) = H_c(\omega) \sum_i W_\psi \ddot{x}_g(a_j, b_i) \hat{\psi}_{a_j, b_i}(\omega) \quad (15)$$

where,

$$H_i(\omega) = \frac{-1}{\omega_i^2 - \omega^2 + 2i\zeta_i \omega_i \omega} \quad (16)$$

and

$$H_c(\omega) = \frac{-1}{\omega_c^2 - \omega^2 + 2i\zeta_c \omega_c \omega} \quad (17)$$

are the frequency domain transfer functions for the impulsive and the convective responses of the fluid in the tank. The expressions for wavelet transform coefficients of  $x_i$  and  $x_c$  may now be used to find out the peak coefficients of the hydrodynamic pressure on the tank wall and the shear and overturning moment at the tank base.

#### 4. Hydrodynamic Pressure, Base Shear and Overturning Moment

The expressions for hydrodynamic pressure,  $P_H$ , on the tank wall, the shear,  $Q_{BS}$ , at the tank base, and the overturning moment,  $M_B$ , immediately at a section above the tank base, for a fixed-base tank at any instant of time  $t$ , are given in Appendix B. On using the wavelet-based representation,  $P_H$ ,  $Q_{BS}$  and  $M_B$  may be written as

$$P_H(t) = \sum_i \sum_j \frac{K'' \Delta b}{a_j} W_\psi P_H(a_j, b_i) \psi_{a_j, b_i}(t) \quad (18)$$

$$Q_{BS}(t) = \sum_i \sum_j \frac{K'' \Delta b}{a_j} W_\psi Q_{BS}(a_j, b_i) \psi_{a_j, b_i}(t) \quad (19)$$

and

$$M_B(t) = \sum_i \sum_j \frac{K'' \Delta b}{a_j} W_\psi M_B(a_j, b_i) \psi_{a_j, b_i}(t) \quad (20)$$

On multiplying both sides of Equations (18), (19) and (20) by  $\hat{\psi}_{a_k, b_l}^*(\omega)$ , using Equation (11), and then on taking Fourier transform of both sides, the relationships of wavelet coefficients of hydrodynamic pressure, base shear and base moment with the wavelet coefficients of ground acceleration are obtained as

$$\sum_i W_\psi P_H(a_j, b_i) \hat{\psi}_{a_j, b_i}(\omega) = \tau_{PH} \sum_i W_\psi \ddot{x}_g(a_j, b_i) \hat{\psi}_{a_j, b_i}(\omega) \quad (21)$$

$$\sum_i W_\psi Q_{BS}(a_j, b_i) \hat{\psi}_{a_j, b_i}(\omega) = \tau_{BS} \sum_i W_\psi \ddot{x}_g(a_j, b_i) \hat{\psi}_{a_j, b_i}(\omega) \quad (22)$$

and

$$\sum_i W_\psi M_B(a_j, b_i) \hat{\psi}_{a_j, b_i}(\omega) = \tau_{MB} \sum_i W_\psi \ddot{x}_g(a_j, b_i) \hat{\psi}_{a_j, b_i}(\omega) \quad (23)$$

where, the transfer functions for hydrodynamic pressure,  $\tau_{PH}$ , for base shear,  $\tau_{BS}$ , and for overturning base moment,  $\tau_{MB}$ , are

$$\tau_{PH} = -\omega^2 \rho_l R [C_i(z) H_i(\omega) + C_c(z) H_c(\omega)] \quad (24)$$

$$\tau_{BS} = -\omega^2 [m_i H_i(\omega) + m_c H_c(\omega)] \quad (25)$$

and

$$\tau_{MB} = -\omega^2 [m_i h_i H_i(\omega) + m_c h_c H_c(\omega)] \quad (26)$$

The above expressions for  $\tau_{PH}$ ,  $\tau_{BS}$  and  $\tau_{MB}$  may be non-dimensionalised by dividing by  $\rho_l g H$ ,  $m_l g$  and  $m_l g H$ , respectively, in order to get the transfer functions of the coefficients of hydrodynamic pressure,  $C_{PH}$ , base shear,  $C_{BS}$ , and base moment,  $C_{MB}$ , respectively. The expressions for the transfer functions of non-dimensional pressure, shear and moment coefficients, denoted by  $\tau_{CPH}$ ,  $\tau_{CBS}$  and  $\tau_{CMB}$  respectively, are given by

$$\tau_{CPH} = \frac{-\omega^2}{\frac{H}{R} g} [C_i(z)H_i(\omega) + C_c(z)H_c(\omega)] \quad (27)$$

$$\tau_{CBS} = \frac{-\omega^2}{g} [\gamma_i H_i(\omega) + \gamma_c H_c(\omega)] \quad (28)$$

and

$$\tau_{CMB} = \frac{-\omega^2}{g} [\gamma_i \frac{h_i}{H} H_i(\omega) + \gamma_c \frac{h_c}{H} H_c(\omega)] \quad (29)$$

where,  $\gamma_i$  and  $\gamma_c$  respectively represent the ratios of impulsive and convective liquid masses with respect to the total liquid mass. On taking expectation of the square of the amplitude of both sides of Equation (21), integrating over  $\omega$ , and on using the normalized relationship for the proposed L-P basis function (Basu and Gupta, 1998), we get

$$\sum_i E[|W_\psi P_H(a_j, b_i)|^2] = \sum_i E[|W_\psi \ddot{x}_g(a_j, b_i)|^2] \int_{-\infty}^{\infty} |\tau_{PH}(\omega)|^2 |\hat{\psi}_{a_j, b_i}(\omega)|^2 d\omega \quad (30)$$

The time-localization property of the wavelet coefficients may be used to find out the instantaneous energy of the hydrodynamic pressure coefficient response,  $C_{PH}$ , over an interval  $\Delta b$  at the instant  $t = b_i$ , corresponding to the band with dilation factor,  $a_j$ . This instantaneous energy is given by

$$\int_{-\infty}^{\infty} E[|(C_{PH})_i^j(\omega)|^2] d\omega = \frac{K'' \Delta b}{a_j} E[|W_\psi \ddot{x}_g(a_j, b_i)|^2] \int_{-\infty}^{\infty} |\tau_{CPH}(\omega)|^2 |\hat{\psi}_{a_j, b_i}(\omega)|^2 d\omega \quad (31)$$

and the instantaneous power spectral density function (PSDF) of the pressure coefficient can be written as (see Basu and Gupta (1998))

$$S_{C_{PH}}(\omega) = \sum_j \frac{E[|(C_{HP})_i^j(\omega)|^2]}{\Delta b} = \sum_j \frac{K''}{a_j} E[|W_\psi \ddot{x}_g(a_j, b_i)|^2] |\tau_{CPH}(\omega)|^2 |\hat{\psi}_{a_j, b_i}(\omega)|^2 \quad (32)$$

The moments of instantaneous PSDF of  $C_{PH}(t)$  are needed to be evaluated in order to obtain more information about the statistics of the response process,  $P_H(t)$ . The expressions for the zeroth, first and second moments of the PSDF in this case are given as

$$m_0 |_{t=b_i} = \sum_j K' E[|W_\psi \ddot{x}_g(a_j, b_i)|^2] I_{0,j}(\omega_n, \zeta) \quad (33)$$

$$m_1 |_{t=b_i} = \sum_j K' E[|W_\psi \ddot{x}_g(a_j, b_i)|^2] I_{1,j}(\omega_n, \zeta) \quad (34)$$

and

$$m_2 |_{t=b_i} = \sum_j K' E[|W_\psi \ddot{x}_g(a_j, b_i)|^2] I_{2,j}(\omega_n, \zeta) \quad (35)$$

with

$$I_{0,j} = \int_{\pi/a_j}^{\sigma\pi/a_j} |\tau_{CPH}|^2 d\omega \quad (36)$$

$$I_{1,j} = \int_{\pi/a_j}^{\sigma\pi/a_j} |\tau_{CPH}|^2 \omega d\omega \tag{37}$$

$$I_{2,j} = \int_{\pi/a_j}^{\sigma\pi/a_j} |\tau_{CPH}|^2 \omega^2 d\omega \tag{38}$$

and

$$K' = \frac{K''}{\pi(\sigma - 1)} \tag{39}$$

The expected value of the largest peak,  $E(x_{(1)})$ , of hydrodynamic pressure coefficient can be obtained from the expressions in Appendix C. The peak values of the base shear coefficients and the overturning base moment coefficients can be found out in a similar way, as was done for the peak hydrodynamic pressure coefficients.

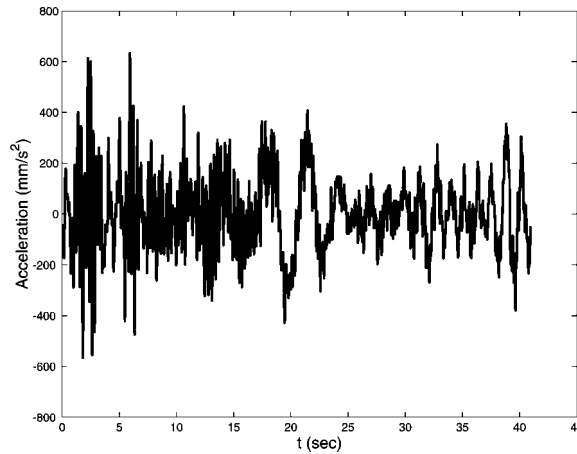


Fig. 2 Acceleration time history synthetically generated by SYNACC for the 1989 Loma Prieta earthquake motion at Dumbarton bridge site

### COMPARISON BETWEEN TIME HISTORY SIMULATIONS AND WAVELET FORMULATION RESULTS

An ensemble of seventeen accelerograms corresponding to the ground motion process for the Loma Prieta earthquake, 1989 at Dumbarton Bridge site near Coyote Hills has been generated artificially by using the SYNACC (Synthetically Generated Accelerogram) program (Wong and Trifunac, 1979; Lee and Trifunac, 1985, 1987, 1989; Trifunac, 1990). One such accelerogram is shown in Figure 2. The parameters considered are the same as those taken by Gupta and Trifunac (1993). A single realization of accelerogram from the generated ensemble has been used to calculate the wavelet coefficients, and thus to characterize the process by the functionals of the calculated wavelet coefficients (see Chatterjee and Basu (2001)). The discretization parameters for calculating the wavelet coefficients,  $\Delta b$  and  $\sigma$ , are chosen as 0.02 and  $2^{\frac{1}{4}}$  respectively, leading to 22 frequency bands (with  $j$  varying between -17 to 4) at 2047 instants of time. The local averages of wavelet coefficients squared are used to represent the ensemble averaged wavelet coefficients squared. In this technique, corresponding to each frequency band, the total duration of seismic signal is divided into a number of stretches, each stretch having duration equal to the central time period,  $\frac{4\pi}{\frac{\pi}{a_j} + \frac{\sigma\pi}{a_j}}$ , of the corresponding frequency band. The wavelet coefficients are squared and then averaged over each stretch to represent the value of  $E[W_{\psi}^2 \ddot{x}_g(a_j, b_i)]$  uniformly over the stretch as

$$E[W_{\psi}^2 \ddot{x}_g(a_j, b_i)] = \frac{(1+\sigma)\Delta b}{4a_j} \sum_{k=\frac{4a_j m}{(1+\sigma)\Delta b}}^{\frac{4a_j(m+1)}{(1+\sigma)\Delta b}} W_{\psi}^2 \ddot{x}_g(a_j, b_k), \quad m = 0, 1, 2, \dots \quad (40)$$

To verify the reliability of local averaging method, the pseudo-spectral acceleration (PSA) response of a linear single degree of freedom (SDOF) system for two different levels of damping, 1% and 5%, has been simulated by direct time history integrations for each realization of the ensemble of accelerograms. Similar computations are carried out for peak coefficients for hydrodynamic pressure, base shear, and base moment of the 2-DOF system in the present study, for different heights of liquid in the tank and for various height-radius ratios. For these computations, the values of different parameters assumed constant are as follows. The damping ratio,  $\zeta_i$ , of the impulsive liquid mass (water being considered for the present study) is assumed to be the same as that of the tank material which is equal to 5%. The values of Young's modulus of elasticity and density of the tank material are  $2.1 \times 10^6 \text{ kg/cm}^2$  and  $7850 \text{ kg/m}^3$ , respectively. The damping ratio,  $\zeta_c$ , of the convective mode of the liquid is assumed to be 1%. The tank wall thickness to tank radius ratio,  $h/R$ , is assumed to be 0.001. Correspondingly, the value of  $C_i$  in Equation (3) can be chosen from Table (II) of Veletsos and Tang (1990).

The term  $C_c(z)$  represents the dimensionless function defining the distribution of first sloshing mode of hydrodynamic pressure. For lateral seismic excitation, the expression for  $C_c(z)$  (see Veletsos and Tang (1990)) for calculating pressure on tank wall is given by Equation (B.4). The results obtained from time history integrations are averaged over the ensemble, and are compared with those obtained from the wavelet-based stochastic analysis proposed in this paper, while using the locally averaged wavelet coefficient functionals. Figures 3 and 4 show the PSA curves for different time periods of the SDOF oscillators at damping ratios 5% and 1%, respectively. The results from stochastic analyses are seen to compare very well with the simulation results. Thus, the above comparisons show that the proposed technique of characterizing the ground motions by processing of a single accelerogram record is satisfactory.

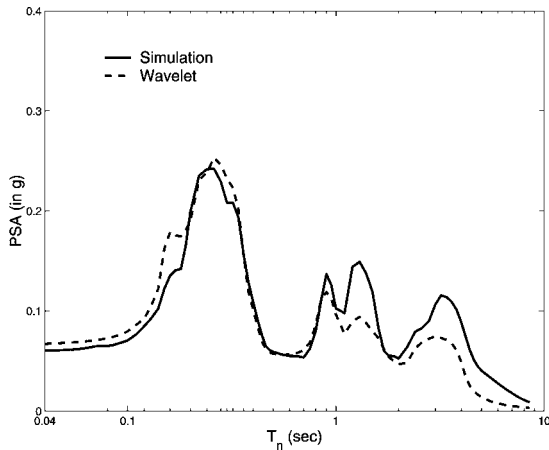


Fig. 3 Comparison of PSA spectra obtained by stochastic-wavelet formulation and ensemble averaging corresponding to a damping ratio of 5%

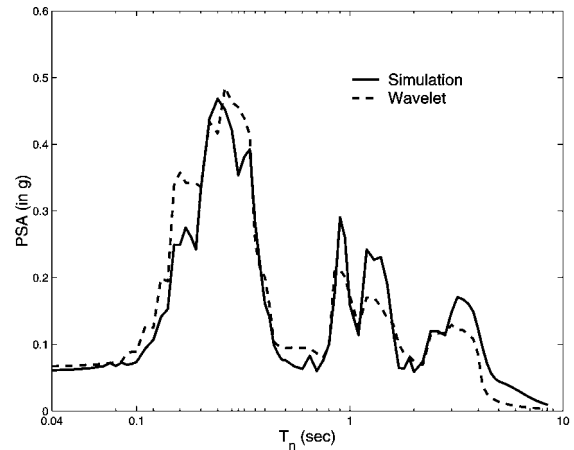


Fig. 4 Comparison of PSA spectra obtained by stochastic-wavelet formulation and ensemble averaging corresponding to a damping ratio of 1%

Figures 5–10 plot the variations of hydrodynamic pressure coefficients at different heights on the tank wall for various heights of liquid in the tank, in case of two different height-radius ratios. Figures 5–7 show satisfactory comparisons of results from time-history and wavelet-based analyses for  $H = 3 \text{ m}$ ,  $7 \text{ m}$  and  $15 \text{ m}$ , respectively, in case of height-radius ratio of 1.0. Figures 8–10 show that the matching between the time-history results and wavelet analyzed results are excellent for  $H = 3 \text{ m}$ ,  $7 \text{ m}$  and  $15 \text{ m}$ , respectively, in case of height-radius 3.0.

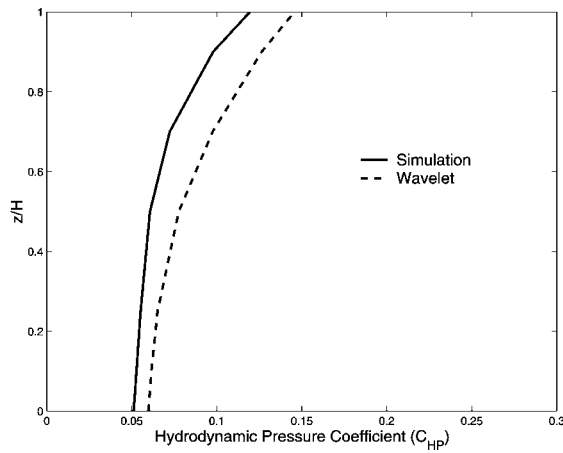


Fig. 5 Variation in hydrodynamic pressure coefficients along tank wall in case of  $H = 3$  m and  $H/R = 1.0$

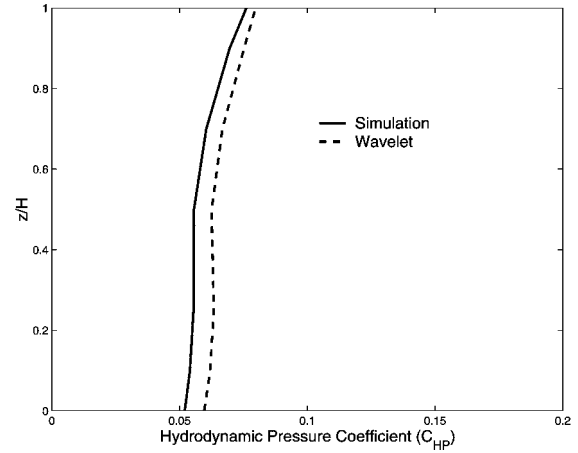


Fig. 6 Variation in hydrodynamic pressure coefficients along tank wall in case of  $H = 7$  m and  $H/R = 1.0$

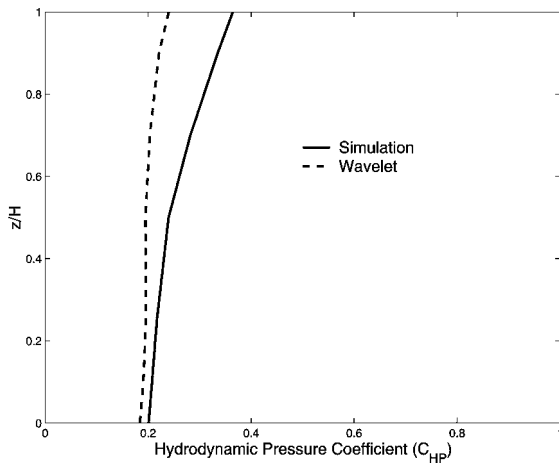


Fig. 7 Variation in hydrodynamic pressure coefficients along tank wall in case of  $H = 15$  m and  $H/R = 1.0$

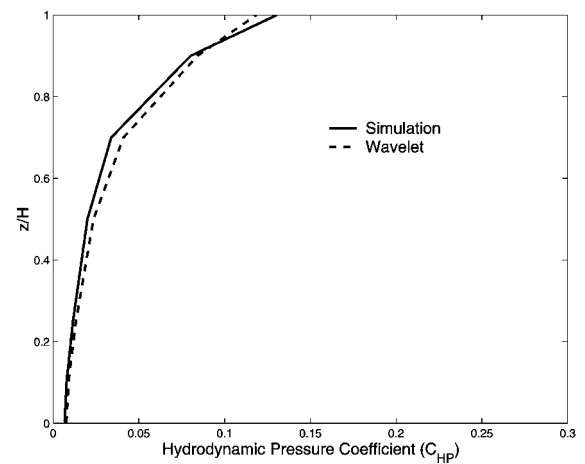


Fig. 8 Variation in hydrodynamic pressure coefficients along tank wall in case of  $H = 3$  m and  $H/R = 3.0$

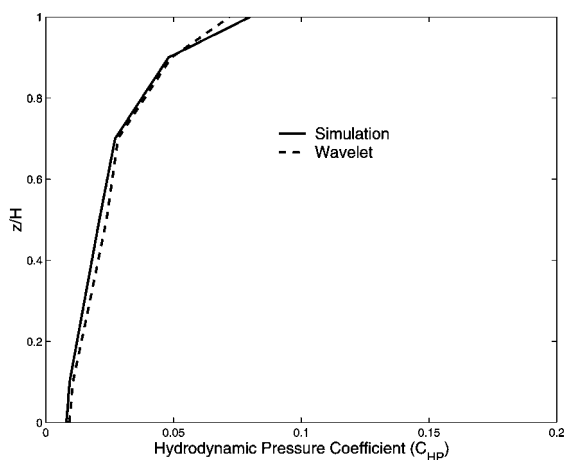


Fig. 9 Variation in hydrodynamic pressure coefficients along tank wall in case of  $H = 7$  m and  $H/R = 3.0$

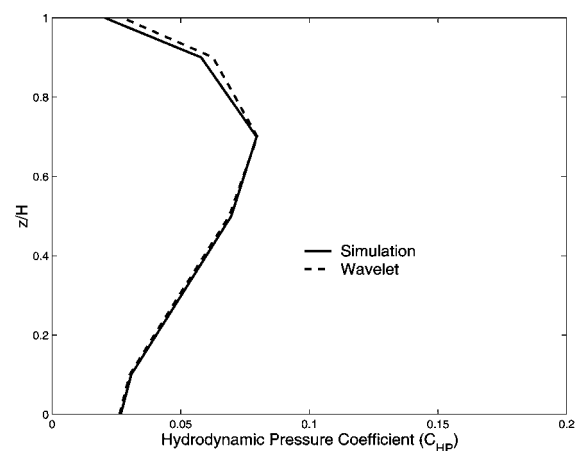


Fig. 10 Variation in hydrodynamic pressure coefficients along tank wall in case of  $H = 15$  m and  $H/R = 3.0$

Figures 11–13 show the variations of base shear coefficients against different tank heights for various height-radius ratios, viz. 0.5, 1.0 and 3.0, respectively. It is observed that reasonably good matching is obtained in case of  $H/R = 1.0$  and 3.0. However, for very broad tanks with  $H/R = 0.5$ , the quality of matching slightly deteriorates. It may be noted that at  $H/R = 0.5$ , the impulsive and convective time periods of most of the tanks lie in that range, for which the matching in PSA responses, as shown in Figures 3 and 4, is also not so close. This may be the reason for slight mismatch in the results of the base shear coefficients at  $H/R = 0.5$ . Similar arguments apply for  $H/R = 1.0$  beyond about  $H = 12$  m and for  $H/R = 3.0$  in the range of  $H = 3.5$  m to 6.5 m, where slight deviations are observed between the averaged time history simulation results and the stochastic analysis results.

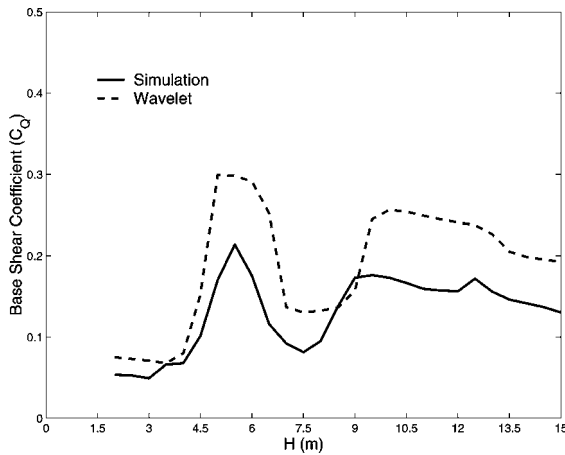


Fig. 11 Variation in base shear coefficients against different liquid heights in the tank in case of  $H/R = 0.5$

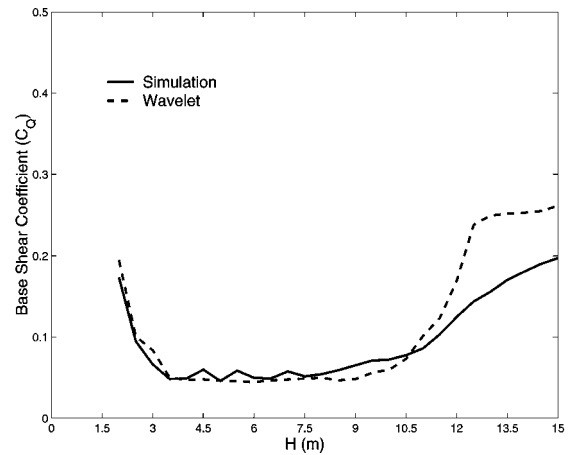


Fig. 12 Variation in base shear coefficients against different liquid heights in the tank in case of  $H/R = 1.0$

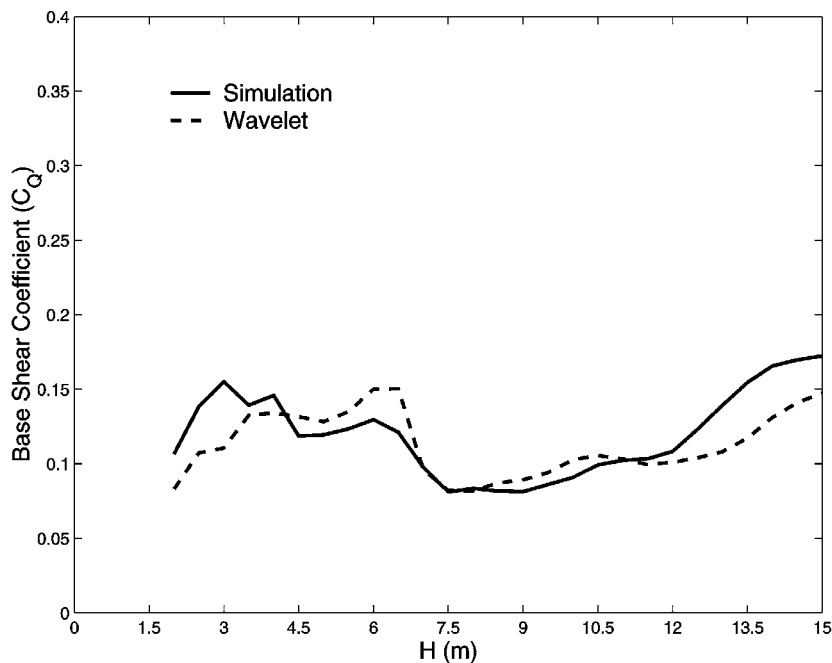


Fig. 13 Variation in base shear coefficients against different liquid heights in the tank in case of  $H/R = 3.0$

Figures 14–16 demonstrate the variation of base moment coefficient with liquid height in the tank for different height-radius ratios, viz. 0.5, 1.0 and 3.0, respectively. The results obtained from wavelet-based stochastic analysis are close to those obtained from the time-history analysis, with the exceptions for the ranges, as in the case of base shear coefficients, caused possibly due to similar reasons.

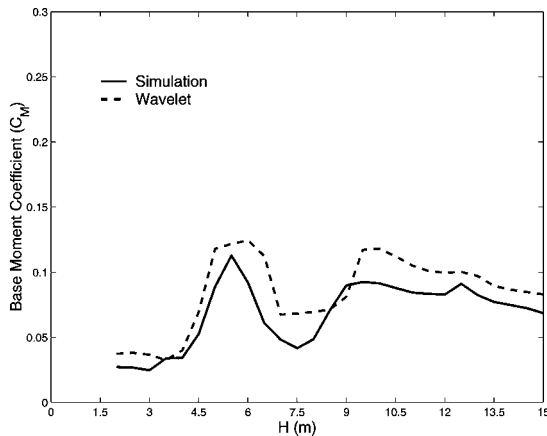


Fig. 14 Variation in base moment coefficients against different liquid heights in the tank in case of  $H/R = 0.5$

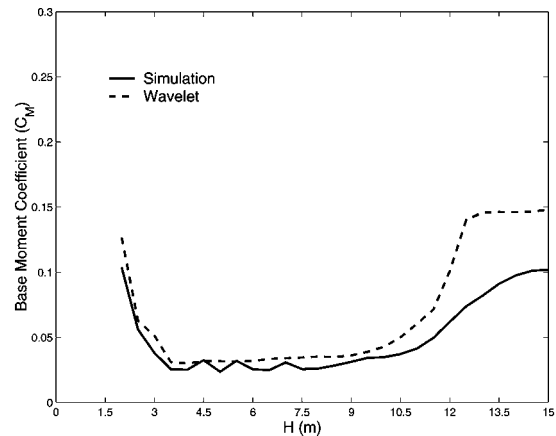


Fig. 15 Variation in base moment coefficients against different liquid heights in the tank in case of  $H/R = 1.0$

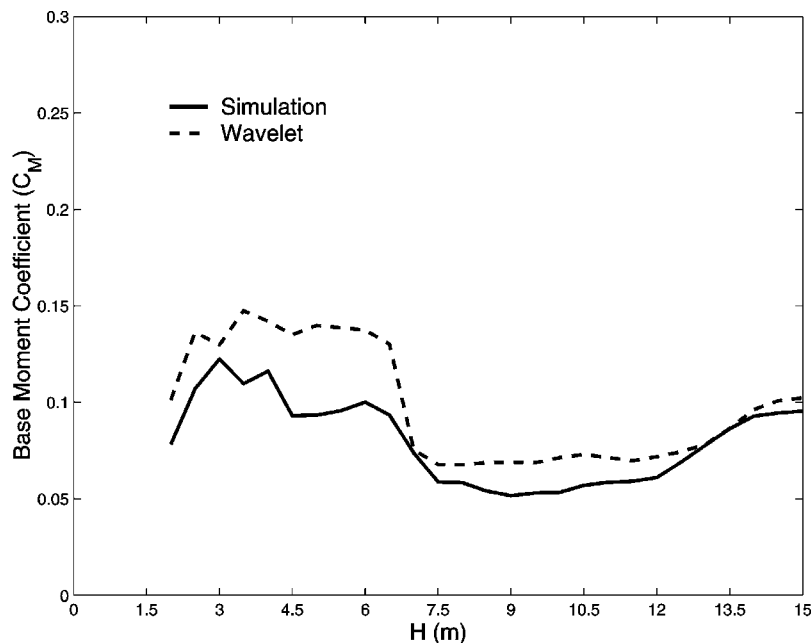


Fig. 16 Variation in base moment coefficients against different liquid heights in the tank in case of  $H/R = 3.0$

**NUMERICAL RESULTS**

A parametric study on the stochastic responses of the tank-fluid system is carried out by the proposed wavelet-stochastic formulation, by varying the liquid height,  $H$ , and the height-radius ratio,  $H/R$ , of the tank. It may be observed from the curves corresponding to the wavelet-based stochastic results in Figures 5–7 that in case of  $H/R = 1.0$ , for smaller tanks (say,  $H = 3$  m), the pressure coefficients sharply increase along the tank wall till the liquid surface is reached; for medium-sized tanks, this variation is gradual, whereas there is a sudden fall in the magnitude of pressure coefficient at the tank surface compared to that at  $0.9H$  when the tank is large (say,  $H = 15$  m). A similar trend is followed in case of slender tanks ( $H/R = 3.0$ ), as can be seen from the plots of the wavelet-based stochastic results in Figures 8–10. In this case, for large tanks (see Figure 10), the pressure coefficients start decreasing beyond a liquid height of about  $0.7H$ . Comparing only those curves in Figures 5–7 which correspond to wavelet-based stochastic analysis, it is revealed that the magnitudes of the pressure coefficients at most of the points on the tank wall for any tank height decrease, if the height-radius ratio of the tanks is increased.

On comparing the stochastically obtained base moment coefficients for various height-radius ratios (from Figures 14–16), the peak value is observed to occur at about  $H = 6$  m and 10 m in cases of broad tanks with  $H/R = 0.5$ , because the respective convective time periods (convective mass is dominant in case of very broad tanks) correspond to peaks in Figure 4. In case of tanks with  $H/R = 1.0$ , high values are observed to occur for very small (say, less than 3.5 m height) or very large (say, with heights greater than 10 m) tanks, because the respective impulsive and convective time periods (both modes contribute more or less equally in this case) correspond to peaks in Figures 3 and 4. For slender tanks ( $H/R = 3.0$ ), larger base moment coefficient values occur when tank heights are less than 6 m. On comparing the curves from Figures 11–13, corresponding to the results obtained from wavelet-based stochastic analysis, similar conclusions can be drawn regarding the variation in base shear coefficients due to change in  $H$  or  $H/R$  ratios.

## CONCLUSIONS

A wavelet-based stochastic formulation for the non-stationary seismic response of fixed-base liquid storage tanks has been presented here. The non-stationary ground motion process has been characterized by the statistical estimates of wavelet coefficients obtained from a single realization of the process. The ‘local averaging’ technique helps in statistical computation of expected values of squared wavelet coefficients from one accelerogram only, and this analytical method is quite useful in those cases where a very few accelerograms are available at hand. However, further improvement in the method of obtaining the expected squared wavelet coefficients is expected to improve the stochastic results. The proposed characterization scheme has been validated with time history simulation results averaged over an ensemble of accelerograms for some specific cases.

The proposed formulation has the advantage over the traditional methods, as this can explicitly account for the frequency and amplitude non-stationarities of the response of tank under seismic excitations, and also can include the modal cross-correlations of the different modes of response of liquid storage tanks. Further, the present approach avoids tedious calculations based on time history simulation for stochastic estimates of the response, particularly when either very few time histories are available at a site or those are difficult to generate from the information available. The proposed approach in general works quite well; however, the success of this partly depends on how well the functionals of wavelet coefficients calculated from few time histories available, characterize the ground motion.

The following conclusions can be drawn on the basis of parametric variations carried out to see the effects on the responses of fixed-base tanks. It has been observed that if height to radius ratio of the tank is increased, the hydrodynamic pressure coefficient gradually decreases for any specific tank height. Generally, the pressure coefficients increase along the height of the tank; however, in case of larger tanks, the pressure coefficients at points situated above around  $0.7H$  on the tank wall show a decreasing trend. The variations of base shear coefficients and overturning base moment coefficients with respect to tank heights follow a similar trend as the pressure coefficients.

## APPENDIX A: WAVELET BASIS

The seismic ground acceleration,  $\ddot{x}_g(t)$ , may be considered to be a process with zero mean, non-stationary Gaussian characteristics. The wavelet transform coefficients,  $W_\psi \ddot{x}_g(a_j, b_i)$  ( $= \frac{1}{|a_j|^{\frac{1}{2}}} \int_{-\infty}^{\infty} \ddot{x}_g(t) \psi \frac{(t-b_i)}{a_j} dt$ ), of this process with respect to a wavelet basis function,  $\psi(t)$ , represent the contribution of the ground motion process in the neighbourhood of discretized time instant  $t = b_i$  and in the frequency band corresponding to the dilation factor  $a_j$ . On assuming  $a_j = \sigma^j$  and  $b_j = (j-1)\Delta b$  (see Basu and Gupta (1998)), one can reconstruct back the ground acceleration signal as

$$\ddot{x}_g(t) = \sum_i \sum_j \frac{K'' \Delta b}{a_j} W_\psi \ddot{x}_g(a_j, b_i) \psi_{a_j, b_i}(t) \quad (\text{A.1})$$

where,

$$K'' = \frac{2}{4\pi C_\psi} \left( \sigma - \frac{1}{\sigma} \right) \tag{A.2}$$

and

$$C_\psi = \int_{-\infty}^{\infty} \frac{|\hat{\psi}(\omega)|^2}{|\omega|} d\omega < \infty \tag{A.3}$$

The value for  $\sigma$  in Eq. (A.2) has been chosen as  $2^{\frac{1}{4}}$  (Basu and Gupta, 1998) for reasonable representation of most of the ground motions. In Eq. (A.3), the function  $\psi(\cdot)$  is the ‘basic’ or the ‘mother’ wavelet with the Fourier transform,  $\hat{\psi}(\omega) = \frac{1}{\sqrt{2\pi}} \int_{-\infty}^{\infty} \psi(t) e^{-i\omega t} dt$ . The non-stationary seismic base acceleration process with instantaneous Gaussian distribution may be characterized by the expected value of the wavelet coefficient squared, i.e.  $E[\{W_\psi \ddot{x}_g(a_j, b_i)\}^2]$ .

In this study, Littlewood-Paley (L-P) basis function characterized by its Fourier transform

$$\begin{aligned} \hat{\psi}(\omega) &= \frac{1}{\sqrt{2(p-1)\pi}}, \quad \pi \leq |\omega| \leq p\pi \\ \hat{\psi}(\omega) &= 0, \quad \text{otherwise} \end{aligned} \tag{A.4}$$

has been used. The time domain representation of this wavelet is given by

$$\psi(t) = \frac{1}{\pi \sqrt{\sigma-1}} \frac{\sin \sigma \pi t - \sin \pi t}{t} \tag{A.5}$$

where,  $\sigma = p$ . A brief review on the wavelet transform, its usage in representation of seismic base acceleration, and on L-P basis function may be found in Basu and Gupta (2000b).

**APPENDIX B: HYDRODYNAMIC PRESSURE, BASE SHEAR AND BASE MOMENT**

The expressions for hydrodynamic pressure,  $P_H(t)$ , on the tank wall, the shear,  $Q_{BS}(t)$ , and the moment,  $M_B(t)$ , just above the tank base are respectively given as

$$P_H(t) = \rho_l R [C_i(z)x_i(t) + C_c(z)x_c(t)] \tag{B.1}$$

$$Q_{BS}(t) = m_i x_i(t) + m_c x_c(t) \tag{B.2}$$

and

$$M_B(t) = m_i h_i x_i(t) + m_c h_c x_c(t) \tag{B.3}$$

The heights  $h_i$  and  $h_c$  give the locations of impulsive and convective masses respectively, at which they should be placed to give the correct moments at a section immediately above the tank base. The term  $C_i(z)$  in Equation (B.1) denotes the coefficient for impulsive component of hydrodynamic pressure. The term  $C_c(z)$  represents the dimensionless function defining the distribution of first sloshing mode of hydrodynamic pressure. For lateral seismic excitation, the expression for  $C_c(z)$  (see Veletsos and Tang (1990)) for calculating pressure on tank wall may be written as

$$C_c(z) = \frac{2}{\lambda_1^2 - 1} \frac{\cosh(\lambda_1 \frac{z}{R})}{\cosh(\lambda_1 \frac{H}{R})} \tag{B.4}$$

**APPENDIX C: EXPECTED LARGEST PEAK OF A STOCHASTIC PROCESS**

The expected value of the largest peak of a stochastic process can be obtained as

$$E(x_{(1)}) = \int_0^1 P_T^{-1}(u) du \quad (C.1)$$

In Equation (C.1),  $P_T(x)$  ( $=u$ ) is the probability that the process  $|x_i(t)|$  remains below the level  $x$  within the time interval  $[0, T]$ , and is given by

$$P_T(x) = \exp\left[-\int_0^T \alpha(t) dt\right] \quad (C.2)$$

where,

$$\alpha(t) \Big|_{t=b_i} = \frac{\Omega_i}{\pi} e^{-\frac{x^2}{2\sigma_i^2}} \frac{1 - \exp(-\sqrt{\pi/2}[\Lambda_i(t)]^{1.2} \frac{x}{\sigma_i})}{1 - \exp(-\frac{x^2}{2\sigma_i^2})} \quad (C.3)$$

The terms  $\Lambda_i$  and  $\Omega_i$  in Equation (C.3) represent respectively the band-width parameter and instantaneous rate of zero crossings. The expressions for  $\Lambda_i$  and  $\Omega_i$  may be written as (see Basu and Gupta (1998))

$$\Lambda_i = \sqrt{1 - \frac{m_1^2 \Big|_{t=b_i}}{m_0 \Big|_{t=b_i} m_2 \Big|_{t=b_i}}} \quad (C.4)$$

and

$$\Omega_i = \sqrt{\frac{m_2 \Big|_{t=b_i}}{m_0 \Big|_{t=b_i}}} \quad (C.5)$$

## REFERENCES

1. Basu, B. and Gupta, V.K. (1997). "Non-stationary Seismic Response of MDOF Systems by Wavelet Transform", *Earthquake Engrg. Struct. Dynamics*, Vol. 26, pp. 1243–1258.
2. Basu, B. and Gupta, V.K. (1998). "Seismic Response of SDOF Systems by Wavelet Modelling of Nonstationary Process", *J. Engrg. Mech., ASCE*, Vol. 124, No. 10, pp. 1142–1150.
3. Basu, B. and Gupta, V.K. (1999). "Wavelet-Based Analysis of the Non-stationary Response of a Slipping Foundation", *J. Sound Vib.*, Vol. 222, No. 4, pp. 547–563.
4. Basu, B. and Gupta, V.K. (2000a). "Wavelet-Based Non-stationary Response Analysis of a Friction Base-Isolated Structure", *Earthquake Engrg. Struct. Dynamics*, Vol. 29, pp. 1659–1676.
5. Basu, B. and Gupta, V.K. (2000b). "Stochastic Seismic Response of Single-Degree-of-Freedom Systems through Wavelets", *Engineering Structures*, Vol. 22, pp. 1714–1722.
6. Chatterjee, P. and Basu, B. (2001). "Nonstationary Seismic Response of Tanks with Soil Interaction by Wavelets", *Earthquake Engrg. Struct. Dynamics*, Vol. 30, pp. 1419–1437.
7. Ghanem, R. and Romeo, F. (2000). "A Wavelet Based Approach for the Identification of Linear Time-Varying Dynamical Systems", *Journal of Sound and Vibration*, Vol. 234, No. 4, pp. 555–576.
8. Ghanem, R. and Romeo, F. (2001). "A Wavelet Based Approach for Model and Parameter Identification of Nonlinear Systems", *International Journal of Nonlinear Mechanics*, Vol. 36, No. 5, pp. 835–859.
9. Gupta, V.K. and Trifunac, M.D. (1993). "A Note on the Effects of Ground Rocking on the Response of Buildings during 1989 Loma Prieta Earthquake", *Earthq. Eng. Eng. Vib.*, Vol. 13, No. 2, pp. 12–28.
10. Haroun, M.A. (1983). "Vibration Studies and Tests of Liquid Storage Tanks", *Earthquake Engg. Struct. Dynamics*, Vol. 12, pp. 179–206.
11. Haroun, M.A. and Tayel, M.A. (1985). "Response of Tanks to Vertical Seismic Excitations", *Earthquake Engrg. Struct. Dynamics*, Vol. 14, pp. 583–595.
12. Housner, G.W. (1963). "The Dynamic Behaviour of Water Tanks", *Bull. Seismological Soc. Amer.*, Vol. 2, pp. 381–387.

13. Koh, H.M., Kim, K.J. and Park, J.-H. (1998). "Fluid-Structure Interaction Analysis of 3-D Rectangular Tanks by a Variationally Coupled BEM-FEM and Comparison with Test Results", *Earthquake Engrg. Struct. Dynamics*, Vol. 27, pp. 109–124.
14. Lee, V.W. and Trifunac, M.D. (1985). "Torsional Accelerograms", *Soil Dyn. Earthq. Eng.*, Vol. 3, pp. 132–139.
15. Lee, V.W. and Trifunac, M.D. (1987). "Rocking Strong Earthquake Accelerograms", *Soil Dyn. Earthq. Eng.*, Vol. 2, pp. 75–89.
16. Lee, V.W. and Trifunac, M.D. (1989). "A Note on Filtering Strong Motion Accelerograms to Produce Response Spectra of Specified Shape and Amplitude", *Euro. Earthq. Eng.*, Vol. III, No. 2, pp. 38–45.
17. Mukherjee, S. and Gupta, V.K. (2002a). "Wavelet-Based Characterization of Design Ground Motions", *Earthquake Engrg. Struct. Dynamics*, Vol. 31, pp. 1173–1190.
18. Mukherjee, S. and Gupta, V.K. (2002b). "Wavelet-Based Generation of Spectrum-Compatible Time-Histories", *Soil Dyn. Earthq. Eng.*, Vol. 22, No. 12, pp. 817–822.
19. Peek, R. (1988). "Analysis of Unanchored Liquid Storage Tanks under Lateral Loads", *Earthquake Engrg. Struct. Dynamics*, Vol. 17, pp. 1087–1100.
20. Peek, R. and Jennings, P.C. (1988). "Simplified Analysis of Unanchored Tanks", *Earthquake Engrg. Struct. Dynamics*, Vol. 17, pp. 1073–1085.
21. Trifunac, M.D. (1990). "Curvograms of Strong Ground Motions", *J. Eng. Mech.*, ASCE, Vol. 6, pp. 1426–1432.
22. Veletsos, A.S. and Yang, J.Y. (1977). "Earthquake Response of Liquid Storage Tanks", in "Advances in Civil Engineering through Engineering Mechanics", *Proc. Eng. Mech. Specialty Conf.*, ASCE, Raleigh, N.C., U.S.A., pp. 1–24.
23. Veletsos, A.S. and Tang, Y. (1990). "Soil-Structure Interaction Effects for Laterally Excited Liquid Storage Tanks", *Earthquake Engrg. Struct. Dynamics*, Vol. 19, pp. 473–496.
24. Wong, H.L. and Trifunac, M.D. (1979). "Generation of Artificial Strong Motion Accelerograms", *Earthquake Engrg. Struct. Dynamics*, Vol. 8, pp. 509–527.
25. Yeh, C.-H. and Wen, Y.K. (1990). "Modeling of Nonstationary Motion and Analysis of Inelastic Structural Response", *Struct. Safety*, Vol. 1-4, pp. 281–298.
26. Zeldin, B. and Spanos, P. (1996). "Random Field Representation and Synthesis Using Wavelet Bases", *Jour. Appl. Mech.*, ASME, Vol. 63, pp. 946–952.